npj Precision Oncology

https://doi.org/10.1038/s41698-026-01332-1

Article in Press

FLT3-SYK inhibitor and Ixazomib combination impact HOXA and oxidative stress control by β-catenin, SQSTM1 and NRF2 in AML

Received: 12 November 2024

Accepted: 6 February 2026

Cite this article as: Pasupuleti, S.K., Rangaraju, S., Layer, J. *et al.* FLT3-SYK inhibitor and Ixazomib combination impact HOXA and oxidative stress control by β-catenin, SQSTM1 and NRF2 in AML. *npj Precis. Onc.* (2026). https://doi.org/10.1038/s41698-026-01332-1

Santhosh Kumar Pasupuleti, Sravanti Rangaraju, Justin Layer, Kanaka Sai Ram Padam, Larry D. Cripe, Hamid Sayar, Katie J. Sargent, Jill Weisenbach, Heiko Konig, Huda Salman, Baskar Ramdas, Lakshmi Reddy Palam, Lindsey D. Mayo, Irum Khan, Utpal P. Davé, H. Scott Boswell & Reuben Kapur

FLT3-SYK Inhibitor and Ixazomib Combination Impact HOXA and Oxidative Stress Control by β-Catenin, SQSTM1 and NRF2 in AML

Santhosh Kumar Pasupuleti[1,#], Sravanti Rangaraju[2,3,#], Justin Layer[2,#], Kanaka Sai Ram Padam[1], Larry D Cripe[2], Hamid Sayar[2], Katie J Sargent[4], Jill Weisenbach[2,5], Heiko Konig[2], Huda Salman[6], Baskar Ramdas[1], Lakshmi Reddy Palam[1], Lindsey D Mayo[1], Irum Khan[7], Utpal Dave[2,8,10], H Scott Boswell[2,8,10,$] and Reuben Kapur[1,9,*]

[1]Herman B Wells Center for Pediatric Research, Department of Pediatrics, Indiana University School of Medicine, Indianapolis, IN 46202, USA.

[2]Indiana University and Melvin and Bren Simon Cancer Center, Indianapolis, IN 46202, USA.

[3]Hematology/Oncology at the Kirklin Clinic University of Alabama Birmingham, Birmingham, AL, USA.

[4]IU Health Partners, Indianapolis, IN, USA.

[5]Indiana University School of Medicine, Indianapolis, IN 46202, USA.

[6]Indiana Cancer Research Center, Brown Center for Immunotherapy, Indianapolis, IN, USA.

[7]Northwestern University School of Medicine, Chicago, IL, USA.

[8]Hematology/Oncology, Indiana University School of Medicine, Indianapolis, IN, USA.

[10]Veterans Affairs Medical Center, Indianapolis, IN, USA.

[9]Department of Microbiology & Immunology, Indiana University School of Medicine, Indianapolis, IN 46202, USA.

[#]Contributed equally

[$]Diseased

***Corresponding author:**

Reuben Kapur, Ph.D.

Professor of Pediatrics

Herman B Wells Center for Pediatric Research

Indiana University School of Medicine

1044 W. Walnut Street, R4-168

Indianapolis, IN 46202

317-274-4658

rkapur@iu.edu

Running Title: Duality of AML Resistance Signaling

Abstract

Acute myeloid leukemia (AML) is sustained by oncogenic signaling and stress-adaptive networks that enable proliferative sustenance and therapeutic resistance. Transcriptomic profiling of AML blasts revealed upregulation of *FLT3*, *SYK*, *HOXA9/10*, and *CTNNB1* with elevated oxidative phosphorylation (OXPHOS). Proteasome inhibition induced phosphorylation-dependent ubiquitination and nuclear export of β-catenin, triggering stress signaling (p62/SQSTM1/c-JUN/NRF2) and apoptosis in *FLT3*^{ITD} mutant AML blasts. Dual targeting of FLT3/SYK (TAK-659) and the proteasome (Ixazomib) showed strong synergy across genetically defined AML subsets, irrespective of *FLT3* mutant status. In *Tet2*$^{-/-}$;*Flt3*^{ITD} AML-transplanted mice models, combination therapy markedly reduced leukemic burden, restored CD45.1^{+} normal hematopoiesis, corrected disease-associated cytopenias, and normalized hematopoietic stem and progenitor composition. In our phase I/II clinical trial, this combination therapy induced rapid leukemic clearance, early transcriptional silencing of HOXA/FLT3/NRF2 programs, and durable hematologic responses in refractory AML patients. These findings define a therapeutically targetable axis linking FLT3/SYK/β-catenin signaling to stress adaptation, provide a mechanistic basis for combinatorial targeting in high-risk AML. Trial registration: NCT04079738, Date of registration 03 September 2019.

Introduction

Resistance to AML therapy has been attributed in part to the presence of leukemic stem cells (LSCs), whose abundance in patients correlates with elevated expression of HOXA and HOXB cluster genes and their cofactor MEIS1[1,2,3]. AML effectors associated with high HOX/MEIS1 expression include mutant FLT3 and SYK kinases, mutant nucleophosmin (NPM1), and KMT2A-rearranged leukemias, with FLT3- and NPM1-mutant AMLs each accounting for approximately 30% of cases[2–4]. In contrast, karyotypically defined core-binding factor (CBF) AMLs display low LSC content, lack HOX and MEIS1 expression, and generally respond favorably to chemotherapy, achieving high cure rates[2,5]. NPM1-mutant AMLs, in the absence of co-mutations that confer poor prognosis, frequently exhibit robust HOX expression yet remain highly responsive to chemotherapy, achieving durable remissions[1,5]. This apparent paradox was clarified by the finding that the transcription factor FOXM1 whose elevated expression predicts poor outcomes across diverse AML genotypes is sequestered in the cytoplasm of NPM1-mutant blasts. The cytoplasmic trapping of FOXM1 by the C-terminally mutated NPM1 renders FOXM1 transcriptionally inactive, thereby attenuating its oncogenic function[6].

Importantly, the long-standing association between chemoresistance and LSC burden alone has been challenged[7]. This highlights the need to consider additional molecular contributors such as FOXM1 and its cooperating pathways. FOXM1 is a central component of an oxidative-stress-responsive transcriptional program that activates NRF2 (nuclear factor erythroid 2-related factor 2) and p62/SQSTM1. Notably, NRF2 and p62 form a self-reinforcing positive feedback loop[8–11]. NRF2 is both necessary and sufficient for sustaining expression of all ten nuclear-encoded cytochrome c oxidase (COX) subunit genes, thereby maintaining oxidative phosphorylation (OXPHOS)[12–14]. High p62/SQSTM1 expression is likewise associated with poor outcomes in AML, owing in part to its function as a signaling scaffold for MAPK and NF-κB pathways[15]. Through its reciprocal relationship with NRF2 where p62 promotes NRF2 stability and NRF2 drives p62 transcription this signaling hub amplifies cellular defense mechanisms against both oncogenic and therapy-induced stress. Moreover, p62/SQSTM1 levels are further augmented by cytokine signaling from the bone-marrow microenvironment[16–18].

Upon interpretation of two successive clinical trials previously performed[19], addition of Bortezomib to a FLT3/RAF inhibitor and HDAC inhibitor significantly enhanced clinical response in the 3-drug cohort compared to FLT3/RAF inhibitor and HDAC inhibitor treatment alone. Bortezomib has been shown to induce β-catenin ubiquitination through stress-related activation of the E3 ligase Siah-1, leading to nuclear exclusion and loss of transcriptional activity[20,21]. Additionally, phosphorylation

at residues Ser31, Ser37, Thr41, and Ser45 regulates β-catenin compartmentation and transcriptional silencing[22], and HOXA cluster gene transcription involves β-catenin through both TCF-dependent and TCF-independent cis-elements linked with c-JUN[23–26].

Based on these insights, we hypothesized that overcoming leukemic resistance requires dual targeting of HOX-driven transcriptional programs and the high-OXPHOS metabolic state characteristic of refractory AML. To achieve this, we employed a combinatorial strategy using the FLT3/SYK inhibitor TAK-659 together with Ixazomib, a proteasome inhibitor known to induce stress-mediated, E3 ligase- and casein kinase 1α-dependent inactivation of β-catenin.

Results

Differential expression in AML blasts highlights FLT3/SYK/HOX driven proliferation, enhanced OXPHOS, and suppressed lymphocyte signaling:

The transcriptomic analysis of AML patient's blast samples (n=26) compared with healthy donor samples (n=10) (GEO: GSE9476) identified 3,519 upregulated and 2,759 downregulated genes (**Figure 1A**). Notably, AML blasts showed marked overexpression of the receptor tyrosine kinase *FLT3*, non-receptor kinase *SYK*, developmental regulators *HOXA9*/*HOXA10*, stress-response gene *c-JUN*, and β-catenin pathway components *CTNNB1* and *CSNK1A1* (**Figure 1B**). KEGG pathway analysis revealed significant enrichment of PI3K–AKT, RAP1, RAS, and WNT signaling, as well as pathways involved in hematopoietic lineage regulation, AML pathogenesis, and transcriptional misregulation (**Figure 1C**). Gene ontology analysis showed activation of mitochondrial electron transport, ribosomal biogenesis and aerobic respiration, whereas T-cell receptor signaling, innate immune responses, and lymphocyte-mediated immune responses were suppressed in AML blasts (**Figure 1D**). GSEA hallmark analysis further demonstrated enhanced G2/M checkpoint, MYC targets, and oxidative phosphorylation, with reduced apoptosis (**Figure 1E–F, Supplemental Figure 1**). Collectively, these data define AML pathogenesis as driven by coordinated activation of FLT3/SYK/HOXA and β-catenin signaling programs that promote leukemic cell proliferation and survival.

AML patient blast samples from *FLT3* mutant AML revealed Bortezomib or Ixazomib induced posttranslational modification (PTM) on β-Catenin, affecting nuclear export:

The Phosphorylated (Ser33/Ser37/Thr41) β-catenin (inactive) was noted to be elevated in the cytosol in the Bortezomib (65nM) treated AML blasts (patient #2929 and #2952) in alone or in

combination with R406 (330nM) compared to the DMSO treated control cells. This is accompanied by the reduced or undetected phospho-β-catenin in the nucleus. The non-phosphorylated (Ser33/Ser37/Thr41) β-catenin (active) form was notably increased upon Bortezomib treated AML blasts cells in the cytosol. However, the levels were undetected in the nucleus **(Figure 1G-H)** indicating attenuated posttranslational modification of the reduced non-phospho (Ser45) β-catenin (active) in the nucleus compared to the control. This suggests an impairment in ubiquitination and a subsequent effect on nuclear translocation in AML blast cells treated with Bortezomib, either alone or in combination.

Bortezomib induced an increase in cytoplasmic p62/SQSTM1 and nuclear phosphorylated (Ser73) c-JUN, consistent with the induction of cellular stress response. Notably, these stress-associated effects were antagonized by co-treatment with the FLT3/SYK inhibitor R406, indicating a signaling interplay between stress response pathways and FLT3/SYK activity **(Figure 1G-H)**. Functionally, the Bortezomib and R406 combination induced the strongest apoptotic response (35% early and late apoptosis by propidium iodide staining) and significantly reduced procaspase 4 and non-canonical p52/RELB NFκB levels, molecules associated with poor-risk AML[27] **(Supplemental Figure 1)**. A modest reduction in the long half-life antiapoptotic protein BCL-2 was also observed, consistent with NFκB role as a transcriptional regulator. Together, these findings identify Bortezomib-induced post-translational modification and nuclear export of β-catenin as a mechanistic event associated with enhanced apoptotic response and HOXA downregulation in FLT3-ITD AML blasts, providing a molecular basis for the improved clinical response observed with Bortezomib-containing combinations[19].

Together, these findings establish that Bortezomib induces post-translational modification and nuclear export of CTNNB1 (β-catenin), alongside activation of a p62/c-JUN mediated stress program, which sensitizes *FLT3*^{ITD} AML blasts to apoptosis. The enhanced apoptotic response and suppression of NFκB signaling provide a mechanistic basis for the improved clinical activity observed in Bortezomib-containing therapeutic combinations[19], highlighting β-catenin modulation as a key molecular event in therapeutic response.

Ixazomib suppresses nuclear β-catenin signaling via enhanced phosphorylation and cytoplasmic accumulation by ubiquitin-tagging:

The non-phospho (active) β-catenin, which is not targeted for ubiquitination, showed increased accumulation in both the cytosolic and nuclear fractions in control samples, indicating its nuclear

localization and transcriptional activity. Upon treatment with TAK-659 (250nM), Ixazomib (100nM), or their combination, the non-phospho β-catenin levels were markedly reduced in the cytosolic fraction. In the nucleus, ixazomib alone and to a similar extent, the combination reduced non-phospho β-catenin, while TAK-659 alone had no effect, suggesting that ixazomib specifically suppresses active β-catenin signaling. In contrast, phospho–β-catenin (Ser33/Ser37/Thr41), which could be tagged for ubiquitination and proteasomal degradation, showed reduced cytosolic levels following TAK-659 treatment, but increased levels with Ixazomib alone or in combination. The elevated phospho–β-catenin in the cytoplasm, with a concomitant corresponding reduction in the nuclear fraction, indicates enhanced tagging for ubiquitination and degradation due to PTM on Ser33/Ser37/Thr41 **(Figure 2A)**. Consistently, immunoprecipitation of total β-catenin confirmed the presence of ubiquitination marks (indicated by the **marks) in Ixazomib-treated cells, similar to the findings noted in the MV4-11 cells treated with the Ixazomib **(Figure 2B)**. By contrast, the Cereblon-4 activator, CC-90009 did not reveal a similar ubiquitin-marked cytoplasmic species and did not reduce nuclear content of β-Catenin. These observations are consistent with the 3T3 cell lysate transduced with the recombinant β-catenin, used an experimental positive control. This effect correlated with increased p62/SQSTM1 protein expression in Ixazomib-treated cells, suggesting that Ixazomib induces β-catenin degradation, shifting β-catenin from its active to inactive state.

p62/SQSTM1 modulates c-JUN, NRF2, and β-Catenin signaling, revealing a regulatory interplay with SYK in AML cells:

Knockdown in MV4-11 cells of c-JUN significantly reduced nuclear phospho (Ser73) c-JUN levels, confirming efficient depletion of the transcriptionally active phosphorylated form, but did not affect protein levels of p62/SQSTM1 or NFE2L2 (NRF2). In contrast, siRNA-mediated knockdown of p62/SQSTM1 led to a marked reduction in phospho (Ser73) c-JUN in both cytoplasmic and nuclear fractions, accompanied by a decrease in NRF2 protein levels **(Figure 2C)**, consistent with p62's established role in facilitating NRF2 stabilization through sequestration of KEAP1 and modulation of stress-responsive transcriptional programs[28]. Knockdown of CTNNB1 (β-catenin) reduced expression of SYK, whereas SYK knockdown reciprocally diminished CTNNB1 expression, revealing a bidirectional regulatory relationship between SYK signaling and β-catenin stability. Furthermore, depletion of p62/SQSTM1 led to reduced NRF2 expression but increased levels of non-phospho (active) β-catenin, suggesting that p62 may facilitate β-catenin inactivation through stress-induced signaling. Conversely, SYK knockdown reduced non-phospho β-catenin levels, indicating its role in maintaining active β-catenin signaling **(Figure 2D)**. Collectively, these

findings uncover a regulatory axis linking p62/SQSTM1/NRF2/c-JUN stress signaling with SYK/β-catenin crosstalk, supporting a coordinated network that sustains oncogenic signaling in AML progression[29].

Combination of TAK-659 and Ixazomib reduces leukemic burden and restores normal hematopoiesis in wild-type (WT) mice transplanted with *Tet2*$^{-/-}$;*Flt3*^{ITD} AML cells

To evaluate the therapeutic efficacy of dual inhibition of FLT3/SYK and the proteasome, we assessed the combined effects of TAK-659 and Ixazomib in *Tet2*$^{-/-}$;*Flt3*^{ITD} (TF) mutant AML mice transplanted into wild-type (WT) recipients. A competitive bone marrow transplantation (BMT) was performed using a 1:1 mixture of TF (CD45.2^{+}) and age-matched BoyJ (CD45.1^{+}) bone marrow cells. Eight weeks post-transplantation, recipient mice were treated with TAK-659 (100 mg/kg, oral, days 1–21), Ixazomib (2 mg/kg, oral, days 1, 8, 15, and 21), either individually or in combination, alongside vehicle controls (**Figure 2E**). After 21 days of treatment, mice were sacrificed and analyzed. Combination therapy led to a marked re-emergence of normal CD45.1^{+} WT cells in the peripheral blood (PB) and bone marrow (BM), accompanied by a significant reduction in leukemic TF CD45.2^{+} cells (**Figure 2F,G**). This treatment also corrected disease-associated hematologic abnormalities, including elevated white blood cell counts and increased frequencies of neutrophils and monocytes, while restoring normal lymphocyte levels compared to vehicle or single-agent groups (**Figure 3A**). In the BM, dual TAK-659 and Ixazomib treatment substantially reduced the proportion of leukemic myeloid cells (Gr-1^{+}/CD11b^{+}) (**Figure 3B**) and significantly decreased the frequency of Lin^{-}Sca1^{+}c-Kit^{+} (LSK) relative to controls (**Figure 3C**). Furthermore, the combination regimen reduced granulocyte macrophage progenitors (GMPs; c-Kit^{+}/CD16/32^{+}/CD34^{+}) while enhancing megakaryocyte erythroid progenitors (MEPs), suggesting a partial restoration of normal hematopoietic differentiation (**Figure 3D**). Overall, combined TAK-659 and Ixazomib therapy effectively reduces leukemic burden, restores normal hematopoietic balance, and reverses stem/progenitor cell abnormalities associated with *Tet2*$^{-/-}$;*Flt3*^{ITD} -driven AML.

Elevated *HOXA*, *FLT3*, and *NRF2* expression predicts poor remission and early relapse in AML

Gene expression analysis of the CBF^{+ve} control sample revealed no detectable levels of *HOXA9/10, MEIS1, SQSTM1, NRF2, BCL2, NQO1,* or *FLT3*, while only low basal levels of c-*JUN*, *SYK*, and *RELB* were present. In contrast, expression profiling of AML blasts from eleven *de novo* or relapsed patients prior to therapy, stratified by their mutational landscape

(Supplemental Table 1), demonstrated marked heterogeneity reflective of clinical outcomes **(Figure 4A)**. Except for patient #3302 (noncanonical *FLT3* Y842C + *MLL-PTD*, successfully treated with third-generation FLT3 inhibitor, induction chemotherapy, and allogeneic transplant), all patients with blast expression of *FLT3*, *BCL2*, *HOXA*, *SQSTM1*, and *NRF2* exceeding 3.5 $\log_{10}$ fold relative to the CBF^{+ve} sample failed to achieve durable remissions following induction and consolidation therapy and/or transplant **(Figure 4A)**.

Gene expression profiles in response to therapy was segregated into the good and poor prognosis groups by the progression-free survival event (≥3 years)[30] (**Figure 4B and Supplemental Table 1**) showed significantly decreased expression of *HOXA9, FOXM1, NFE2L2, p62/SQSTM1,* and *RELB* in the good prognosis group compared to the poor prognosis patient group **(Figure 4B)**. Notably, patient #3238 (*NPM1* mutant, *FLT3*-TKD) with low *HOXA9* expression achieved long-term remission after induction and consolidation, whereas all but the aforementioned patient #3302 in the high NRF2 expression subgroup experienced early relapse or refractory disease.

Additional clinical observations further reinforce the biological significance of these expression programs. Patients #3271 (early relapse, rescued post-transplant) and #3274 (durable remission after induction, consolidation, and transplant) showed reduced *HOXA9/10* expression, while patient #3238 (PFS/OS >4.5 years) exhibited a similar low HOXA9/10 profile, likely driven by mutant *NPM1* without involvement of NRF2 or p62/SQSTM1 dysregulation[31–33]. Conversely, patient #3263 (*FLT3-ITD, MLL-PTD, DNMT3A* mutant) representative of resistant AML exhibited a high OXPHOS and oxidative stress response signature, with markedly elevated *p62/SQSTM1, NRF2, NQO1, FLT3,* and *HOXA9* levels and failed induction therapy with Cytarabine, Idarubicin, and Midostaurin. This transcriptional profile was recapitulated in OCI-AML3 cells, which harbor *NPM1, NRAS,* and *DNMT3A* mutations, and showed high *HOXA9/10*, *JUN-B, SYK, SQSTM1,* and *RELB* expression, mirroring patient blast characteristics and underscoring the link between these oncogenic and stress-adaptive pathways and poor therapeutic outcomes (**Figure 4C**).

Mutational landscape determines differential therapeutic sensitivity on *FLT3* Dependency and stress-adaptive reprogramming in AML

Ixazomib treatment at clinically relevant concentrations (100nM) had minimal anti-proliferative effect on patient #3263 AML blasts (harboring $FLT3^{ITD}$, *MLL-PTD*, and *DNMT3A* mutations). However, its combination with the dual SYK/FLT3 inhibitor TAK-659 (250nM) resulted in strong cooperative activity even at suboptimal (IC_{50}) single-agent doses **(Figure 5A-B)**. Notably, #3263

blasts were also sensitive to TAK-659 monotherapy, reflecting a dependency on *FLT3*^{ITD} and MLL-PTD driven proliferative signaling. The impact of mutational context on drug sensitivity was further evident in patient #3266 (*FLT3*^{ITD}*, NRAS*^{G12D}*, MLL-PTD, RUNX1* mutated), where TAK-659 monotherapy induced limited growth inhibition compared to the Ixazomib with TAK-659 combination **(Figure 5C-D)**. This attenuated response to TAK-659 alone corresponds with low *FLT3* expression and concurrent *NRAS* mutation, consistent with findings by Baccelli, Irène et al. [8] that the cells adapted to *RAS* have less reliance on OXPHOS or are intrinsically hypoxic. By contrast, the *MLL-PTD*/*FLT3* mutant #3263 was dramatically sensitive to TAK-659 (250nM) in alone or in combination treatment with Ixazomib (100nM) (**Figure 5B**).

A distinct sensitivity pattern was observed in patient #3274 (*NRAS*, *ASXL1* mutations, *FLT3* wild-type), whose blasts responded strongly to Ixazomib monotherapy compared to TAK-659 **(Figure 5E–F)**. Likewise, patient #3271 blasts (*FLT3-ITD* with low *FLT3*, *SQSTM1*, *NRF2*, and *FOXM1* expression) exhibited pronounced sensitivity to Ixazomib (IC_{50} = 39.5 nM) and enhanced effects in combination with TAK-659, but intermediate sensitivity to TAK-659 alone (**Supplemental Table 1**). Ixazomib monotherapy elevated *p62/SQSTM1* and *NRF2* protein expression **(Figure 5G)**, whereas the combination markedly suppressed OXPHOS signaling, leading to strong proliferative inhibition at concentrations clinically achievable. This synergy underscores the therapeutic advantage of co-targeting signaling and stress-adaptive pathways in resistant AML clones with high OXPHOS signatures.

In a more in-depth analysis of sensitivity patterns in AML blasts, those without *FLT3* mutations but with *RAS*, *DNMT3A*, *WT1*, *TET2*, *ASXL1* mutations were quite sensitive to Ixazomib (IC50 ranging 39nM-78nM) and displayed varying sensitivity to the combination therapy but were mostly insensitive to TAK-659 alone (**Supplemental Table 1**). Together, these findings highlight Ixazomib therapeutic relevance in genetically defined AML subsets with low *FLT3* dependency or elevated stress-adaptive signatures and provide a strong rationale for combination regimens to enhance efficacy in resistant disease.

Early phase I trial of TAK-659 and Ixazomib demonstrates potent anti-leukemic activity and β-catenin pathway attenuation in AML

Promising activity of the SYK/FLT3 inhibitor TAK-659 was previously reported as a single agent in AML dose-escalation trials, with the strongest efficacy observed in *FLT3*-mutant cohorts compared to *FLT3*-wild-type populations[34]. Consistent with this, in our *in vivo Tet2*$^{-/-}$;*Flt3*^{ITD} AML-

transplanted mouse model, the combination of TAK-659 and Ixazomib markedly reduced leukemic burden, restored normal hematopoiesis, corrected disease-associated cytopenias, and normalized hematopoietic stem and progenitor cell composition. Guided by these preclinical findings, we conducted a pilot Phase I clinical trial evaluating TAK-659 combined with the proteasome inhibitor Ixazomib in relapsed/refractory AML to simultaneously target the FLT3/SYK and β-catenin/SQSTM1/NRF2 stress-adaptation axis. To minimize potential overlapping toxicities and maintain effective pharmacodynamic coverage, TAK-659 was administered at 100 mg orally on days 1-15 of a 21-day cycle, while Ixazomib was given on days 1, 8, and 15 at a starting dose of 2.3 mg orally (Clinical trial #NCT04079738).

The trial enrolled eight patients (one withdrew post-consent), of whom seven were evaluated for hematologic and molecular responses (**Supplemental Table 2**). Six patients were *FLT3*-wild-type and one (patient #CL-1007) carried an *FLT3*^{ITD} mutation previously tested *in vitro* (sample #3263). Overall, combination therapy led to rapid reductions in total WBC counts, peripheral and bone-marrow blast percentages, and bone-marrow cellularity across treated patients by day 15 of cycle 2, indicating potent anti-leukemic activity (**Figure 6A**, and **Table 1**).

Representative data from patients #CL-1003, #CL-1005, and #CL-1007 demonstrate significant hematologic improvement. WBC counts declined from 22, 22, and 17 × 10^3/μL to 1.4, 2.3, and 5.5 × 10^3/μL, respectively. Peripheral-blast percentages were diminished from 79%, 63%, and 51% to 4%, 3%, and 0%, respectively, and bone-marrow cellularity reduced from 90%, 80%, and 80% to 20%, 45%, and 35% (**Figure 6A,B)**. Importantly, these reductions correlated with the suppression of leukemic driver and survival genes. In the *FLT3*^{ITD}-mutant patient (#CL-1007), the response was accompanied by robust downregulation of *SYK*, *JUN*, *SQSTM1*, *RELB*, *NRF2*, *BCL2*, *FLT3*, and *HOXA10*, consistent with inhibition of both the FLT3/SYK and β-catenin/NRF2 stress-response signaling pathways **(Figure 6C)**.

Analysis of nuclear and cytoplasmic fractions from day 4 of treatment revealed reduced phospho (Ser33/Ser37/Thr41) β-catenin in the nucleus corresponding to the increased accumulation in the cytosol, accompanied by distinct posttranslational modification of the protein. These *in vivo* PTMs mirrored the β-catenin phosphorylation and electrophoretic mobility changes seen *in vitro* upon combination treatment, consistent with targeted interference in β-catenin stability and transcriptional activity **(Figure 2A-B)**. β-Catenin is typically targeted for proteasomal degradation through a phosphorylation-dependent ubiquitination process mediated by the destruction complex composed of CK1α, APC, and GSK3β[35]. In patient #CL-1007, this regulatory mechanism

appeared to be further potentiated, as evidenced by increased CK1α levels within the nuclear fraction, indicative of enhanced nuclear export and degradation signaling. This re-localization of CK1α suggests a dampened β-catenin transcriptional program following treatment, consistent with effective pathway attenuation.

Dual SYK/FLT3 and stress-response adaptation drives early molecular response and durable Hematologic improvement in refractory AML

Temporal progression of treatment response in the patient #CL-1005 (refractory case #3306) showed clinical and molecular events due to treatment regimen. Over successive treatment days, WBC counts, peripheral-blast and marrow-blast percentages, and marrow cellularity steadily declined, and the patient achieved a good partial remission (PR) (**Figure 7A** and **Table 1**). This clinical improvement was mirrored by a significant reduction in mRNA expression of *HOXA10*, *BCL2*, *FLT3*, *RELB*, *SQSTM1*, and *NRF2* (**Figure 7B**). Transcriptional repression was evident by day 4 of cycle 1 **(Figure 6C-D)**, preceding major hematologic improvements observed by day 15, highlighting an early molecular response signature.

A similar kinetic pattern was observed in patient #CL-1003 (refractory case #3287), where sustained reductions in WBC counts, peripheral and marrow blasts, and marrow cellularity were documented over the treatment course **(Figure 8A)**. Parallel transcriptional profiling revealed progressive downregulation of leukemic drivers (*HOXA9, HOXA10, FLT3, FOXM1*) and stress-adaptive genes (*SQSTM1, NRF2, JUN, RELB, BCL2*) **(Figure 8B)**. The coordinated decline in these transcriptional networks aligned with hematologic recovery, indicating durable suppression of leukemic signaling pathways and providing mechanistic support for the clinical activity of this combination therapy.

Together, our Phase I/II trial data reveal that dual SYK/FLT3 and proteasome inhibition elicits potent clinical and molecular responses in relapsed/refractory AML, independent of *FLT3* mutational status. The observed concordance between declining leukemic burden and coordinated transcriptional silencing of *HOXA9/HOXA10*, *FLT3*, *FOXM1*, *SQSTM1*, and *NRF2* pathways supports a mechanistic model in which this therapeutic combination simultaneously disrupts proliferative, survival, and redox-adaptation networks crucial for AML persistence.

Discussion

Intensive investigations have identified prognostic subsets of high-risk AML, frequently involving the pairing of type I and type II driver mutations implicated in leukemogenesis[36]. However, the utility of these predictive tools for chemotherapeutic success is often compromised by the presence of additional driver mutations or novel pairings. Significant attention has been directed toward understanding the interaction of distinct mediators derived from class-specific driver mutations affecting *HOXA* gene expression. Notably, recent studies have highlighted Menin-dependent activations of *HOXA* cluster genes by mutant MLL1 and mutant NPM1c, which acts via Menin-dependent wild-type *MLL1*[31]. Compelling evidence for a Menin-independent pathway to *HOXA* expression arises from the activity of *FLT3*^{ITD}, which synergizes with *NUP98-NSD1* in transgenic mouse models to enhance *HOXA* transcription[37]. Additionally, *FLT3*^{ITD} co-expressed with mutant *NPM1* significantly increases *HOXA* transcription in transgenic mice, while mutant *RAS* does not exhibit this effect[38].

Our results align with this molecular framework. We found that AML blasts retaining strong FLT3-ITD signaling and high active β-catenin had reduced sensitivity to the β-catenin targeting proteasome inhibitor Ixazomib. Conversely, blasts lacking FLT3-ITD or those driven by Menin-dependent HOXA activation (mutant NPM1 or mutant RAS cases) were more sensitive to ixazomib-induced apoptosis[1]. For example, the OCI-AML3 cell line (NPM1, NRAS mutated) had low FOXM1 expression. FOXM1 is known to stabilize β-catenin and promote its nuclear localization. Loss of FOXM1 leads to β-catenin ubiquitination and cytoplasmic retention[39].

Consistent with this, OCI-AML3 was highly sensitive to ixazomib and showed increased β-catenin post-translational modifications upon treatment. In glioma models, FOXM1 has been shown to chaperone β-catenin to the nucleus, and both FOXM1 and its partner TBL1 are expressed in myeloid cells[20,39,40]. Thus, in AML subsets with low FOXM1 activity (such as *NPM1* or *RAS* mutated without *FLT3*^{ITD}), β-catenin is more readily inactivated by Ixazomib, correlating with better drug response and longer survival.

We also identified OXPHOS/stress-adaptive pathways as correlates of poor outcome. Blasts from high-risk patients showed upregulation of NRF2, p62/SQSTM1, and related oxidative phosphorylation programs. This aligns with recent reports that AMLs with high mitochondrial activity exhibit therapy resistance. A study reported by Pereira-Martins et al.[41] demonstrated that AML samples with high mitochondrial DNA content have increased mitochondrial mass,

membrane potential, oxygen consumption and BCL-2 expression, all associated with chemoresistance. Clinically, those high-OXPHOS patients had significantly worse outcomes: their 3-year disease-free survival was only 28%, versus 47% for normal-OXPHOS cases[41]. In our cohort, patients whose blasts expressed high NRF2/p62 and HOXA9/10 invariably had early relapse or refractoriness, whereas those with lower stress-gene signatures (even with NPM1 mutations) achieved durable remissions. Our study also documented the adverse prognostic implications of elevated expression levels of stress effectors (*NRF2, p62SQSTM1*) and developmental homeobox transcription factors, *HOXA9/HOXA10*. The OXPHOS pathway is described by *NRF2* and *p62SQSTM1* in a positive feedback relationship[42] involving signals from *Flt3*^{ITD} and *IDH1/IDH2*[43]. These findings underscore that metabolic rewiring (especially enhanced OXPHOS and antioxidant defenses) contributes to AML treatment failure.

Furthermore, AML cells exposed to potentially lethal chemotherapeutic combinations may adapt to develop resistance mechanisms not solely explained by mutational profiles. Common characteristics of intrinsic or acquired treatment resistance in AML include increased mitochondrial mass, heightened oxidative metabolism from fatty acid β-oxidation, and enhanced respiratory enzyme activity[7,8]. These response dependent adaptations are also closely linked to *NRF2*[12,14,42]. A compelling rationale for the observed sensitivity profile, both *in vitro* and *in vivo*, to the combination of Ixazomib and TAK-659 in blasts harboring dominant *FLT3* or *RAS* mutations is attributed to the dual downregulation of *HOXA9/HOXA10* and *NRF2/SQSTM1*. Notably, downregulation of these effectors was associated with remission development *in vivo*. Thus, further investigation into FLT3/SYK inhibition combined with the β-catenin inhibitor Ixazomib is warranted in both *FLT3*-mutant and -wild-type AML settings. Limitations of the study includes a relatively small number of patients, limiting the statistical power to generalize therapeutic outcomes. In addition, the primary AML samples analyzed were heterogeneous in terms of mutational background and relapsed/refractory status, which may have contributed to variability in drug responses. Additionally, while our mechanistic data delineate the interplay between FLT3/SYK signaling, β-catenin regulation, and oxidative stress control, further validation in larger and more genetically defined patient cohorts will be necessary. Collectively, these considerations underscore the importance of future prospective trials designed to integrate molecular profiling with therapeutic response, thereby refining the clinical applicability of this combinatorial approach.

Methods

Differential expression analysis from AML patient samples:

The microarray dataset (GSE9476) consisting of gene expression profile from the AML patient blast samples (n=26) and healthy donors (n=10) was retrieved from the GEO database[44]. Differential gene expression analysis between the groups was performed using interactive webtool, GEO2R (https://www.ncbi.nlm.nih.gov/geo/geo2r/). A log-fold change cutoff of <-0.5 and >+0.5 with p-adjusted <0.05 was considered to be statistically significant. Data was visualized using the EnhancedVolcano R package using R programming language (v4.3, R Core Team, 2020. R: A language and environment for statistical computing. R Foundation for Statistical Computing, Austria).

Functional enrichment analysis:

Gene-set enrichment analysis using the significantly upregulated and downregulated genes was performed to identify the gene ontology (GO) biological process (BP) , Kyoto encyclopaedia of genes and genomes (KEGG) pathways[45], using clusterProfiler R packages[46]. Human molecular signatures database (MSigDB)[47] was accessed to map the cancer hallmarks in the AML blasts using the msigdbr package. Bonferroni-Hochberg correction was applied to determine the statistical significance.

Cell culture conditions:

Primary AML blasts obtained from patients undergoing conventional therapy for either *de novo* or relapsed/refractory AML were obtained prior to the initiation of therapy and had standard cytogenetic and molecular testing recorded. These cells were tested *in vitro* for sensitivity to FLT3/SYK inhibitors (R406 or TAK-659), and to nominal proteasome inhibitors (Bortezomib or Ixazomib). Another aliquot of cells was processed for RNA and subjected to reverse-transcriptase cDNA synthesis for analysis of expression to a panel of 31 genes using GAPDH as control, and core-binding factor (*CBF*$^{+ve}$) AML as calibrator.

Targeted short interfering RNA electroporation:

MV4-11 cells were electroporated using the Amaxa Nucleofector II device (Lonza) according to the manufacturer's protocol. Briefly, 2×10^5 cells were resuspended in 100µL of Nucleofector Solution V and mixed with 100nM of siRNA targeting *p62/SQSTM1*, *c-Jun*, *CTNNB1*, and *SYK* or scramble siRNA (ThermoFisher Scientific). Immediately following electroporation, cells were transferred into pre-warmed McCoy's medium (Gibco) supplemented with 10% fetal bovine serum (FBS) and incubated at 37°C in a humidified 5% CO_2 condition. The nuclear and cytoplasmic

extracts of cells were isolated using NE-PER nuclear and cytoplasmic extraction reagents (Cat. No. 78833, ThermoFisher, USA) following manufacturer's instructions. Knockdown efficiency was assessed by performing immunoblotting.

Mice

All experiments were conducted using male and female mice on a C57BL/6J background. Animals were bred and maintained under specific pathogen-free (SPF) conditions in the animal facility at the Indiana University School of Medicine. Mice were housed under a 12-hour light/dark cycle with unrestricted access to food and water. All procedures were approved by the Laboratory Animal Resource Center of the Indiana University School of Medicine and performed in accordance with institutional animal care guidelines. *Tet2*$^{-/-}$*;Flt3*^{ITD} mutant AML mice were obtained from our in-house colony. Wild-type (WT) control C57BL/6 and Boy/J mice were purchased from the Indiana University School of Medicine Core Facility. The mouse studies were approved by the Indiana University Laboratory Animal Resource Center (Indianapolis, Indiana, USA), and all experiments were conducted at the Laboratory Animal Resource Center according to the protocol.

Competitive bone marrow transplantation

Recipient WT C57BL/6 mice (12 weeks old) were lethally irradiated with a split dose (700 cGy + 400 cGy) one day prior to transplantation. Donor bone marrow (BM) cells (CD45.2^{+}) were harvested from 8-month-old *Tet2*$^{-/-}$*;Flt3*^{ITD} mice and mixed in a 1:1 ratio with age-matched CD45.1^{+} competitor BM cells from Boy/J mice, for a total of 1 × 10^{6} viable cells (500K:500K). The mixed cells were injected intravenously into recipient mice via the tail vein. Peripheral blood (PB) samples were collected every four weeks post-transplantation to assess donor chimerism and engraftment[48].

***In vivo* drug treatment**

For therapeutic experiments, CD45.2^{+} BM cells from *Tet2*$^{-/-}$*;Flt3*^{ITD} donor mice were combined with CD45.1^{+} Boy/J competitor BM cells at a 1:1 ratio (5 × 10^{5} each) and transplanted into lethally irradiated WT recipients as described above. Eight weeks after transplantation, mice were randomly assigned to receive TAK-659 (100 mg/kg, orally, daily on days 1–21), Ixazomib (2 mg/kg, orally, on days 1, 8, 15, and 21), a combination of both agents, or vehicle control.

Peripheral blood counts

Peripheral blood was collected from transplanted mice, and total white blood cell (WBC) counts were measured using an automated hematology analyzer (HT5 Element; Heska) as previously described[48].

Flow cytometry analysis

Flow cytometric immunophenotyping was performed following previously established protocols[48]. Single-cell suspensions from BM and spleen were prepared by mechanical dissociation, followed by red blood cell (RBC) lysis. Cells were washed and resuspended in phosphate-buffered saline (PBS) containing 0.2% bovine serum albumin (BSA) and 10% fetal bovine serum (FBS). For myeloid lineage chimerism analysis in PB, BM, and spleen, the following antibodies were used: CD45.1 APC, CD45.2 FITC, CD11b PE, Gr-1 APC/Cy7, CD3 PE/Cy7, and B220 PerCP/Cy5.5. For hematopoietic stem and progenitor cell (HSPC) analysis, cells were stained with CD45.1 APC, CD45.2 FITC, a lineage-PE cocktail, c-Kit BV785, Sca-1 PE/Cy7, CD48 APC/Cy7, and CD150 PerCP/Cy5.5. For progenitor subset analysis (CMP, GMP, MEP, CLP), cells were labeled with CD45.1 APC, CD45.2 FITC, lineage-PE cocktail, c-Kit BV785, Sca-1 PE/Cy7, CD16/32 APC/Cy7, and CD34 BV421. Samples were acquired on an LSR Fortessa flow cytometer (BD Biosciences) using Diva software and analyzed with FlowJo v10.7.0 (BD Biosciences).

Phase I/II Clinical Trial Design and Patient Selection (ClinicalTrials.gov Identifier: NCT04079738):

This is a Phase I/II clinical trial (Trial registration: NCT04079738, Date of registration 03 September 2019, https://www.clinicaltrials.gov/study/NCT04079738) investigated the combination of TAK-659 and ixazomib in adults with relapsed or refractory acute myeloid leukemia (AML). The study followed a conventional 3 + 3 dose-escalation design, enrolling 3-6 patients per cohort (dose-escalation schema provided in Supplemental Information). Each treatment cycle consisted of 15 consecutive treatment days followed by a 7-day rest period (21-day total cycle length). Bone marrow evaluation for treatment response was performed on Day 15 of each cycle. Responses were defined according to Cheson *et al*.[49]. Patients demonstrating a reduction in bone marrow blasts, but not complete morphological remission after two cycles, were eligible to receive a third cycle (see Supplemental Information).

Patient selection and enrollment:

Adult patients (≥18 years) with histopathologically confirmed relapsed or refractory primary or secondary AML were eligible, excluding those with acute promyelocytic leukemia (APML), complex karyotype, or monosomy 5/7. Eligibility required adequate performance status and hepatic and renal function, as well as provision of written informed consent (see Supplemental Information).

Study Population:

Enrolled patients included both males and females with AML as defined by the World Health Organization, other than APML or cytogenetically complex disease. Eligible cases were further genetically characterized to include normal karyotype, t(MLL), or non-recurrent mutations. For the Phase II portion, patients must have relapsed or refractory disease after no more than two prior chemotherapy regimens and must not have received prior investigational FLT3 inhibitors (previous exposure to midostaurin or gilteritinib was permitted). All patients were required to have adequate organ function and an Eastern Cooperative Oncology Group (ECOG) performance status of 0–2. Patients were excluded if they exhibited clinically significant toxicity from prior therapies, had undergone hematopoietic stem cell transplantation (HSCT) within 60 days of the first dose of TAK-659/ixazomib, or had active graft-versus-host disease requiring ongoing immunosuppressive therapy.

Study approval

The human studies were approved by Indiana University and all experiments were conducted at the Indiana University as per the protocol BTCRC-HEME17-092. For human studies, written informed consent was received prior to participation in accordance with the declaration of Helsinki.

Patient blast cells collection:

Bone marrow (BM) aspirates and peripheral blood (PB) samples were collected from patients within 7 days prior to treatment initiation and again on day 4 of therapy. Mononuclear cells were isolated using Ficoll-Hypaque density gradient centrifugation, and leukemic blast populations were enriched to approximately 80% purity. Cells were washed, counted, and processed immediately for downstream molecular and functional analyses, including RNA extraction, protein profiling, and signaling assays.

Quantitative gene expression analysis:

Quantitative reverse transcription-polymerase chain reaction (qRT-PCR) analysis was performed by targeting 30 AML associated genes with GAPDH as an endogenous control, using low-density TaqMan gene expression array (LDA) format (Cat. No. 4346799, TaqMan Gene Expression Micro Fluidic card, Applied Biosystems, ThermoFisher). Relative mRNA expression was calculated using the $2^{-\Delta\Delta Ct50}$ normalized to the GAPDH, house-keeping gene and fold changes was calculated relative to the CBF^{+} control sample (fusion core-binding factor-positive (*CBF*$^{+ve}$ [inv(16)]), negative for *Flt3*^{ITD}).

Western blot analysis:

The cytosolic or nuclear proteins were extracted using NE-PER nuclear and cytoplasmic extraction reagents (ThermoFisher) from the cultured patient AML blasts, and siRNA treated cells. Total protein concentration was measured using the Pierce BCA Protein Assay Kit (Thermo Scientific, Cat. No. 23225) following the manufacturer's instructions. Equal amounts of protein (20 µg) were separated on 4–20% Novex™ Tris-Glycine Mini Gels (ThermoFisher, Cat. No. XP04205BOX) and transferred to nitrocellulose membranes (Bio-Rad, CA, USA). Membranes were blocked for 1 h with 5% BSA in TBS containing 0.05% Tween-20, then incubated overnight at 4°C with primary antibodies. After washing, membranes were incubated with secondary antibodies for 1 h at room temperature. Signals were detected using Clarity Western ECL substrate (Bio-Rad, Cat. No. 1705061) and visualized with the ChemiDoc imaging system (Bio-Rad). Antibodies used in the study were provided in **Supplemental Table 3**.

Statistical analysis

For comparisons involving more than two groups, one-way analysis of variance (ANOVA) followed by Tukey's post hoc multiple comparisons test was performed. Pairwise comparisons between pre- and post-treatment samples were analyzed using a two-tailed paired t-test, while an unpaired two-tailed t-test was used for comparisons between independent groups. Statistical significance was defined as $p < 0.05$. Significance thresholds were reported as follows, $p<0.05$ (*), $p<0.01$ (**), $p<0.001$ (***), $p<0.0001$ (****), and ns (not significant) for $p \geq 0.05$. Data are presented as mean ± standard deviation (SD), unless otherwise specified.

Data availability statement: The microarray dataset analyzed in this study is publicly available through the NCBI Gene Expression Omnibus (GEO) under accession number GEO: GSE9476.

Acknowledgements

This work was supported by NIH grants R01CA173852, R01CA134777, R01HL146137, and R01HL140961, and Riley Children's Foundation (R.K.), Big Ten Cancer Research Consortium Heme17-092, Galloway Foundation, Department of Veterans Affairs Merit Review (to U.P.D, H.S.B.).

We would also like to dedicate this paper to the memory of our beloved colleague and corresponding author, Dr. H. Scott Boswell, Professor of Medicine, who sadly passed away on April 4th, 2025, during the review process for this manuscript. Dr. Boswell supervised the project, led the associated clinical trial (NCT04079738), and conducted the majority of the experimental work presented here. He also secured the funding that supported this study (Big Ten Cancer Research Consortium Heme17-092, Galloway Foundation, and Department of Veterans Affairs Merit Review). Because his passing occurred after the completion of the research but during manuscript revisions, Dr. Boswell contributed fully to the study design, data generation, and interpretation, and he reviewed earlier versions of the manuscript. However, he was not able to review the final revised version submitted after his passing. We include him as an author in recognition of his indispensable intellectual and scientific contributions.

Author contributions

S.K.P, S.R, and J.L. conceived the study and designed, executed the experiments, analyzed the data, and wrote the manuscript. K.S.R.P performed RNA-seq analysis, analyzed and interpreted the data and critically revised the manuscript. L.D.C, H.S, K.J.S, J.W, H.K, H.S. wrote the manuscript. B.R, L.P. assisted with the experiments. L.D.M, I.K. provided reagents, read the manuscript, and provided critical inputs. H.S.B, R.K, U.D. conceptualized, designed the study, funding acquisition and wrote the manuscript. All authors read and approved the manuscript.

Competing interests

The authors declare no competing interests.

References:

1. Khan, I., Amin, M. A., Eklund, E. A. & Gartel, A. L. Regulation of HOX gene expression in AML. *Blood Cancer J.* **14**, 42 (2024).

2. Eppert, K. *et al.* Stem cell gene expression programs influence clinical outcome in human leukemia. *Nat. Med.* **17**, 1086–1093 (2011).

3. Mohr, S. *et al.* Hoxa9 and Meis1 Cooperatively Induce Addiction to Syk Signaling by Suppressing miR-146a in Acute Myeloid Leukemia. *Cancer Cell* **31**, 549-562.e11 (2017).

4. Puissant, A. *et al.* SYK is a critical regulator of FLT3 in acute myeloid leukemia. *Cancer Cell* **25**, 226–242 (2014).

5. Andreeff, M. *et al.* HOX expression patterns identify a common signature for favorable AML. *Leukemia* **22**, 2041–2047 (2008).

6. Khan, I. *et al.* FOXM1 contributes to treatment failure in acute myeloid leukemia. *JCI insight* **3**, (2018).

7. Farge, T. *et al.* Chemotherapy-Resistant Human Acute Myeloid Leukemia Cells Are Not Enriched for Leukemic Stem Cells but Require Oxidative Metabolism. *Cancer Discov.* **7**, 716–735 (2017).

8. Baccelli, I. *et al.* Mubritinib Targets the Electron Transport Chain Complex I and Reveals the Landscape of OXPHOS Dependency in Acute Myeloid Leukemia. *Cancer Cell* **36**, 84-99.e8 (2019).

9. Rotblat, B., Grunewald, T. G. P., Leprivier, G., Melino, G. & Knight, R. A. Anti-oxidative stress response genes: bioinformatic analysis of their expression and relevance in multiple cancers. *Oncotarget* **4**, 2577–2590 (2013).

10. Han, B. *et al.* Peroxiredoxin I is important for cancer-cell survival in Ras-induced hepatic tumorigenesis. *Oncotarget* **7**, 68044–68056 (2016).

11. Ciamporcero, E. *et al.* Crosstalk between Nrf2 and YAP contributes to maintaining the antioxidant potential and chemoresistance in bladder cancer. *Free Radic. Biol. Med.* **115**, 447–457 (2018).

12. Ongwijitwat, S., Liang, H. L., Graboyes, E. M. & Wong-Riley, M. T. T. Nuclear respiratory factor 2 senses changing cellular energy demands and its silencing down-regulates cytochrome oxidase and other target gene mRNAs. *Gene* **374**, 39–49 (2006).

13. Gleyzer, N., Vercauteren, K. & Scarpulla, R. C. Control of mitochondrial transcription specificity factors (TFB1M and TFB2M) by nuclear respiratory factors (NRF-1 and NRF-2) and PGC-1 family coactivators. *Mol. Cell. Biol.* **25**, 1354–1366 (2005).

14. Scarpulla, R. C. Transcriptional paradigms in mammalian mitochondrial biogenesis and function. *Physiol. Rev.* **88**, 611–638 (2008).

15. Iwadate, R. *et al.* High Expression of SQSTM1/p62 Protein Is Associated with Poor Prognosis in Epithelial Ovarian Cancer. *Acta Histochem. Cytochem.* **47**, 295–301 (2014).

16. Konopleva, M. Y. & Jordan, C. T. Leukemia stem cells and microenvironment: biology and therapeutic targeting. *J. Clin. Oncol. Off. J. Am. Soc. Clin. Oncol.* **29**, 591–599 (2011).

17. Dikic, I. Proteasomal and Autophagic Degradation Systems. *Annu. Rev. Biochem.* **86**, 193–224 (2017).

18. Todoric, J. *et al.* Stress-Activated NRF2-MDM2 Cascade Controls Neoplastic Progression in Pancreas. *Cancer Cell* **32**, 824-839.e8 (2017).

19. Sayar, H. *et al.* Consecutive epigenetically-active agent combinations act in ID1-RUNX3-TET2 and HOXA pathways for Flt3ITD+ve AML. *Oncotarget* **9**, 5703–5715 (2018).

20. Dimitrova, Y. N. *et al.* Direct ubiquitination of beta-catenin by Siah-1 and regulation by the exchange factor TBL1. *J. Biol. Chem.* **285**, 13507–13516 (2010).

21. Matsuzawa, S. I. & Reed, J. C. Siah-1, SIP, and Ebi collaborate in a novel pathway for beta-catenin degradation linked to p53 responses. *Mol. Cell* **7**, 915–926 (2001).

22. Chamorro, M. N. *et al.* FGF-20 and DKK1 are transcriptional targets of beta-catenin and FGF-20 is implicated in cancer and development. *EMBO J.* **24**, 73–84 (2005).

23. Bei, L. *et al.* β-Catenin activates the HOXA10 and CDX4 genes in myeloid progenitor cells. *J. Biol. Chem.* **287**, 39589–39601 (2012).

24. Gan, X. *et al.* Nuclear Dvl, c-Jun, beta-catenin, and TCF form a complex leading to stabilization of beta-catenin-TCF interaction. *J. Cell Biol.* **180**, 1087–1100 (2008).

25. Nateri, A. S., Spencer-Dene, B. & Behrens, A. Interaction of phosphorylated c-Jun with TCF4 regulates intestinal cancer development. *Nature* **437**, 281–285 (2005).

26. Jerković, I. *et al.* Genome-Wide Binding of Posterior HOXA/D Transcription Factors Reveals Subgrouping and Association with CTCF. *PLoS Genet.* **13**, e1006567 (2017).

27. Shanmugam, R. *et al.* A noncanonical Flt3ITD/NF-κB signaling pathway represses DAPK1 in acute myeloid leukemia. *Clin. cancer Res. an Off. J. Am. Assoc. Cancer Res.* **18**, 360–369 (2012).

28. Jaramillo, M. C. & Zhang, D. D. The emerging role of the Nrf2-Keap1 signaling pathway in cancer. *Genes Dev.* **27**, 2179–2191 (2013).

29. Boudria, R. *et al.* Regulatory interplay between Vav1, Syk and β-catenin occurs in lung cancer cells. *Cell. Signal.* **86**, 110079 (2021).

30. Urrutia, S. *et al.* Mortality and relapse dynamics in AML after three years of complete remission. *Leuk. Lymphoma* 1–6 doi:10.1080/10428194.2025.2547984.

31. Uckelmann, H. J. *et al.* Mutant NPM1 Directly Regulates Oncogenic Transcription in Acute Myeloid Leukemia. *Cancer discovery* vol. 13 746–765 at https://doi.org/10.1158/2159-8290.CD-22-0366 (2023).

32. Tiacci, E. *et al.* The NPM1 wild-type OCI-AML2 and the NPM1-mutated OCI-AML3 cell lines carry DNMT3A mutations. *Leukemia* vol. 26 554–557 at https://doi.org/10.1038/leu.2011.238 (2012).

33. Wang, T. *et al.* Gene Essentiality Profiling Reveals Gene Networks and Synthetic Lethal Interactions with Oncogenic Ras. *Cell* **168**, 890-903.e15 (2017).

34. Ueda, K. *et al.* MDMX acts as a pervasive preleukemic-to-acute myeloid leukemia transition mechanism. *Cancer Cell* **39**, 529-547.e7 (2021).

35. van Kappel, E. C. & Maurice, M. M. Molecular regulation and pharmacological targeting of the β-catenin destruction complex. *Br. J. Pharmacol.* **174**, 4575–4588 (2017).

36. Papaemmanuil, E. *et al.* Genomic Classification and Prognosis in Acute Myeloid Leukemia. *N. Engl. J. Med.* **374**, 2209–2221 (2016).

37. Matsukawa, T. *et al.* NUP98::Nsd1 and FLT3-ITD collaborate to generate acute myeloid leukemia. *Leukemia* vol. 37 1545–1548 at https://doi.org/10.1038/s41375-023-01913-0 (2023).

38. Dovey, O. M. *et al.* Molecular synergy underlies the co-occurrence patterns and phenotype of NPM1-mutant acute myeloid leukemia. *Blood* **130**, 1911–1922 (2017).

39. Zhang, N. *et al.* FoxM1 promotes β-catenin nuclear localization and controls Wnt target-gene expression and glioma tumorigenesis. *Cancer Cell* **20**, 427–442 (2011).

40. Choi, H.-K. *et al.* Reversible SUMOylation of TBL1-TBLR1 regulates β-catenin-mediated Wnt signaling. *Mol. Cell* **43**, 203–216 (2011).

41. Pereira-Martins, D. A. *et al.* High mtDNA content identifies oxidative phosphorylation-driven acute myeloid leukemias and represents a therapeutic vulnerability. *Signal Transduct. Target. Ther.* **10**, 222 (2025).

42. Jain, A. *et al.* p62/SQSTM1 is a target gene for transcription factor NRF2 and creates a positive feedback loop by inducing antioxidant response element-driven gene transcription. *J. Biol. Chem.* **285**, 22576–22591 (2010).

43. Stuani, L. *et al.* Mitochondrial metabolism supports resistance to IDH mutant inhibitors in acute myeloid leukemia. *J. Exp. Med.* **218**, (2021).

44. Edgar, R., Domrachev, M. & Lash, A. E. Gene Expression Omnibus: NCBI gene expression and hybridization array data repository. *Nucleic Acids Res.* **30**, 207–210 (2002).

45. Kanehisa, M. & Goto, S. KEGG: kyoto encyclopedia of genes and genomes. *Nucleic Acids Res.* **28**, 27–30 (2000).

46. Yu, G., Wang, L.-G., Han, Y. & He, Q.-Y. clusterProfiler: an R package for comparing biological themes among gene clusters. *OMICS* **16**, 284–287 (2012).

47. Liberzon, A. *et al.* The Molecular Signatures Database (MSigDB) hallmark gene set

collection. *Cell Syst.* **1**, 417–425 (2015).

48. Pasupuleti, S. K. *et al.* Obesity-induced inflammation exacerbates clonal hematopoiesis. *J. Clin. Invest.* **133**, (2023).

49. Cheson, B. D. *et al.* Revised recommendations of the International Working Group for Diagnosis, Standardization of Response Criteria, Treatment Outcomes, and Reporting Standards for Therapeutic Trials in Acute Myeloid Leukemia. *J. Clin. Oncol. Off. J. Am. Soc. Clin. Oncol.* **21**, 4642–4649 (2003).

50. Livak, K. J. & Schmittgen, T. D. Analysis of relative gene expression data using real-time quantitative PCR and the 2(-Delta Delta C(T)) Method. *Methods* **25**, 402–408 (2001).

Figures and Legends

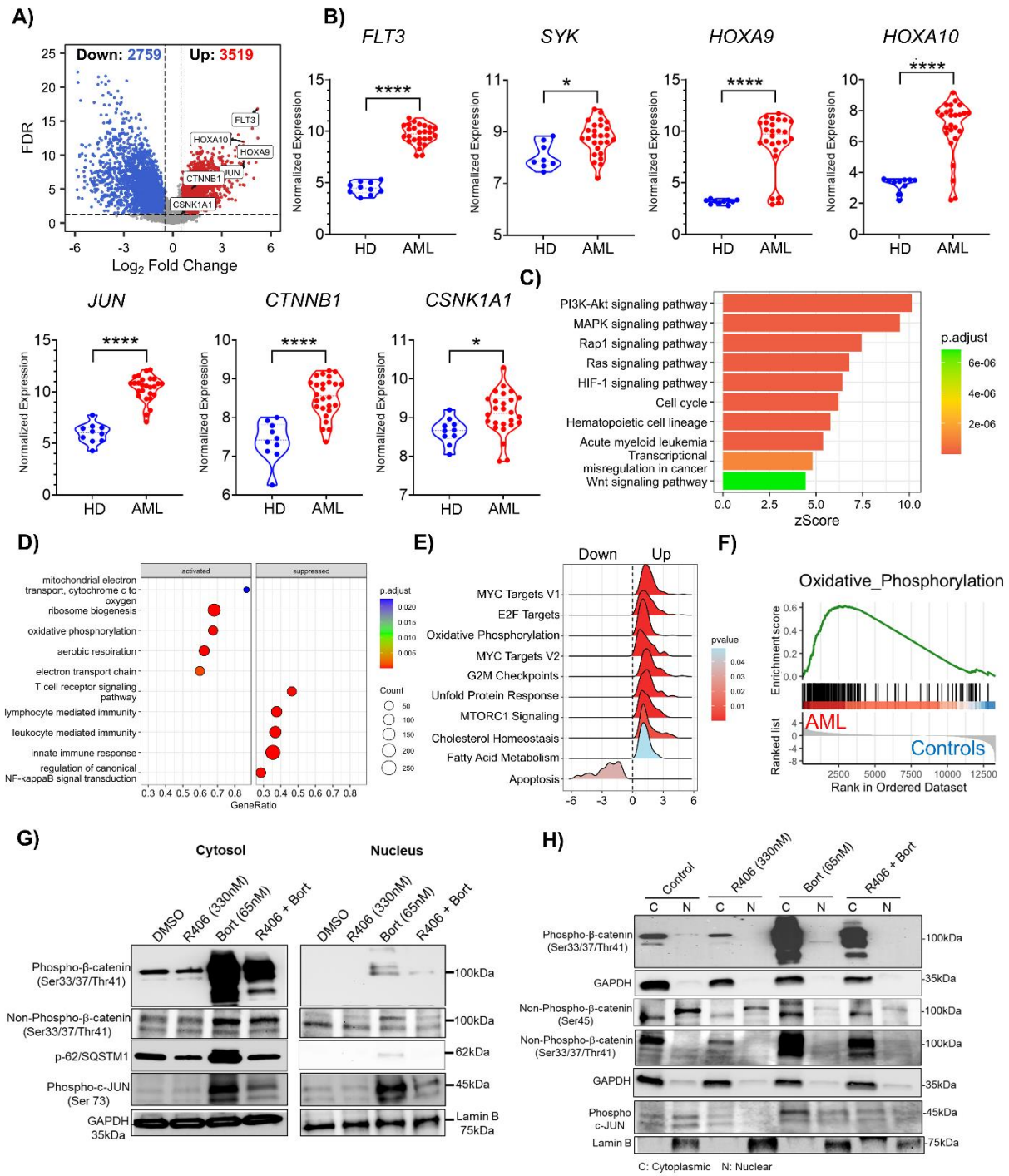

Figure 1

Figure 1: AML blasts exhibit coordinated upregulation of FLT3/SYK/HOXA and β-catenin pathways with enhanced oxidative phosphorylation and stress signaling. A) Differential gene expression analysis (GEO: GSE9476) using GEO2R revealed 2759 downregulated and 3519 upregulated (log2FC>0.5, padj<0.05) genes in the AML patient blasts (n=26) compared to the healthy donors (n=10). **B)** Violin plots depicting the expression of *FLT3*, *SYK*, *HOXA9*, *HOXA10*, *JUN*, *CTNNB1* and *CSNK1A1* across the Healthy donors and AML blasts patient samples. Two-tailed unpaired t-test (*p<0.05, ***p<0.001, ****<0.0001) **C)** Gene set enrichment analysis visualizing the KEGG pathways profiled in the AML blasts compared to the healthy donors. Bonferroni-Hochberg correction (padj<0.05). **D)** Dot plot representing the altered GO-biological processes in the AML blasts patient samples. Bonferroni-Hochberg correction (padj<0.05). **E)** Significant Alteration of GSEA MSigDB hallmarks and, **F)** increased enrichment of oxidative phosphorylation hallmark in the AML blasts. **G-H)** Western blot assay depicting the protein expression profiles of phospho-β-catenin (ser33/37/Thr41), non-phospho β-catenin (ser33/37/Thr41), non-phospho β-catenin (Ser45), phospho c-Jun (Ser73), and p62/SQSTM1 in the cytosolic and nuclear fractions of the **G)** AML #2969 **H)** AML #2952 patient leukemic blasts. GAPDH and Lamin B were used as a loading control for the cytoplasmic and nuclear fractions respectively.

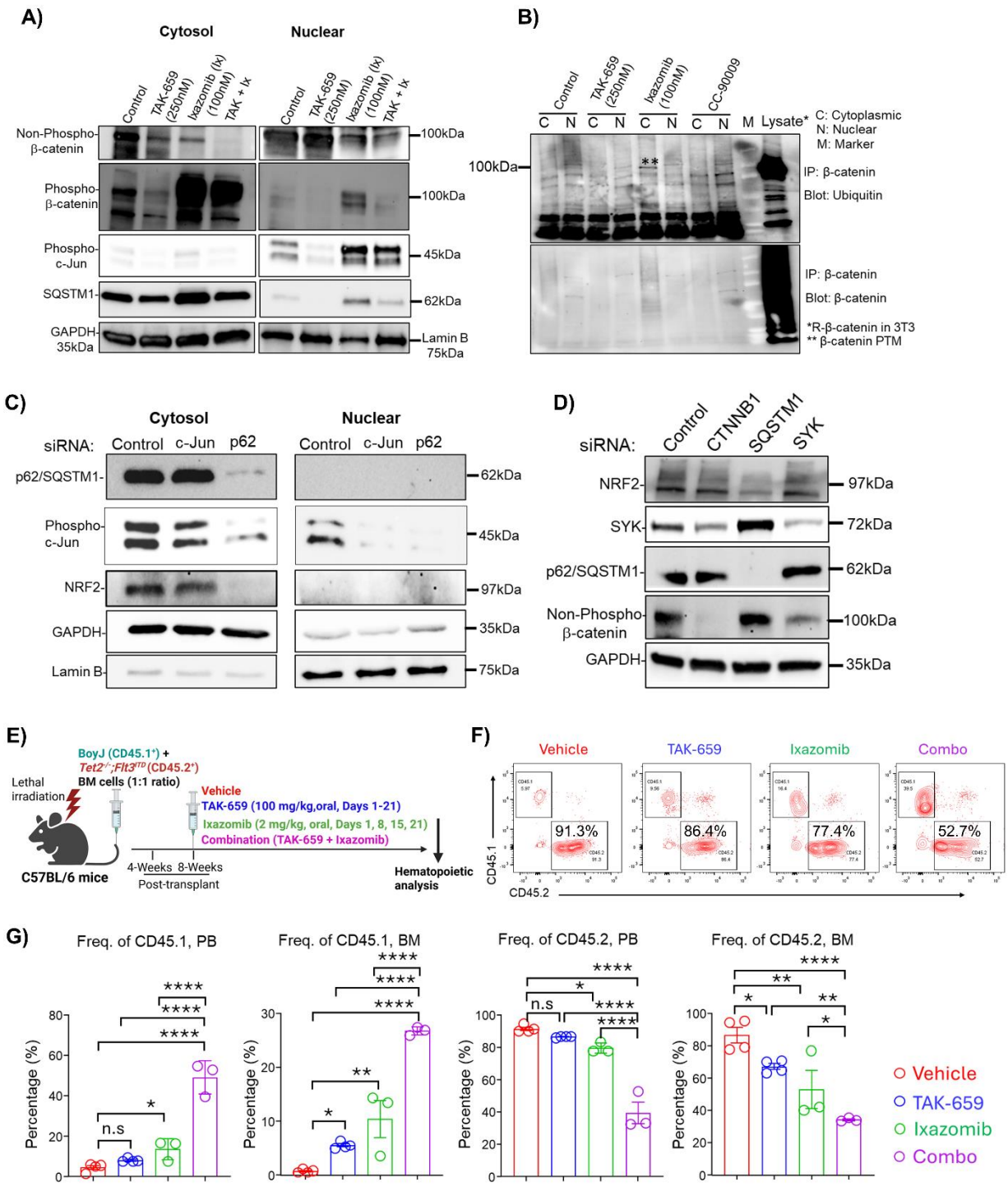

Figure 2

Figure 2: TAK-659 and Ixazomib cooperatively suppress β-catenin, c-Jun, and p62 signaling through SYK-dependent ubiquitination in *FLT3^{ITD}* MV4-11 cells. A-B) *FLT3^{ITD}*

mutant MV4-11 cells were treated with *FLT3/SYK* inhibitor, TAK-659 (250nM) and Ixazomib (100nM), or in a combination of both TAK-659 and Ixazomib at the indicated concentrations. Western blot analysis of phospho-β-catenin (ser33/37/Thr41), non-phospho β-catenin (ser33/37/Thr41), phospho c-Jun (Ser73), and p62/SQSTM1 in the cytosolic and nuclear fractions of MV4-11 cells treated with TAK-659 (FLT3/SYK inhibitor) in alone or in combination with Ixazomib at the indicated concentrations. **B)** The nuclear and cytosolic lysates of MV-411 cells treated overnight with DMSO control, TAK-659 (250nM), or Ixazomib (100nM), or CRBL4 activator – CC900009 (40nM) were immunoprecipitated with β-catenin and immunoblotted for β-catenin or ubiquitin. The recombinant β-catenin within lysate of 3T3 cells transduced with recombinant β-catenin was used as a loading control. (**) indicates ubiquitin marks. Western blot assay using the cell lysates of MV4-11 cells electroporated with the **C)** siRNAs targeting *c-Jun*, *p62*, and **D)** siRNAs targeting beta-catenin *(CTNNB1)*, *SQSTM1* and *SYK*. GAPDH and Lamin B were used as the loading controls. Cells treated with scramble siRNA were used as experimental control. **E)** Experimental design of the competitive bone marrow transplantation (BMT) assay. Lethally irradiated C57BL/6 recipient mice were transplanted with a 1:1 mixture of *Tet2*$^{-/-}$;*Flt3*^{ITD} (TF; CD45.2^{+}) and BoyJ (CD45.1^{+}) bone marrow (BM) cells. Eight weeks post-transplantation, mice were treated with vehicle, TAK-659 (100 mg/kg, oral, daily, days 1-21), Ixazomib (2 mg/kg, oral, days 1, 8, 15, 21), or the combination (TAK-659 + Ixazomib) for 21 days, followed by hematopoietic analysis. **F,G)** Representative flow cytometry plots **(F)** and quantification **(G)** showing frequencies of WT (CD45.1^{+}) and leukemic (CD45.2^{+}) cells in peripheral blood (PB) and BM after treatment. Combination therapy markedly reduced leukemic TF (CD45.2^{+}) cells and promoted re-emergence of normal CD45.1^{+} donor cells. Data are presented as mean ± SEM. Statistical significance was determined by one-way ANOVA with Tukey's multiple-comparison test. *$p < 0.05$, **$p < 0.01$, ***$p < 0.001$, ****$p < 0.0001$; n.s. not significant.

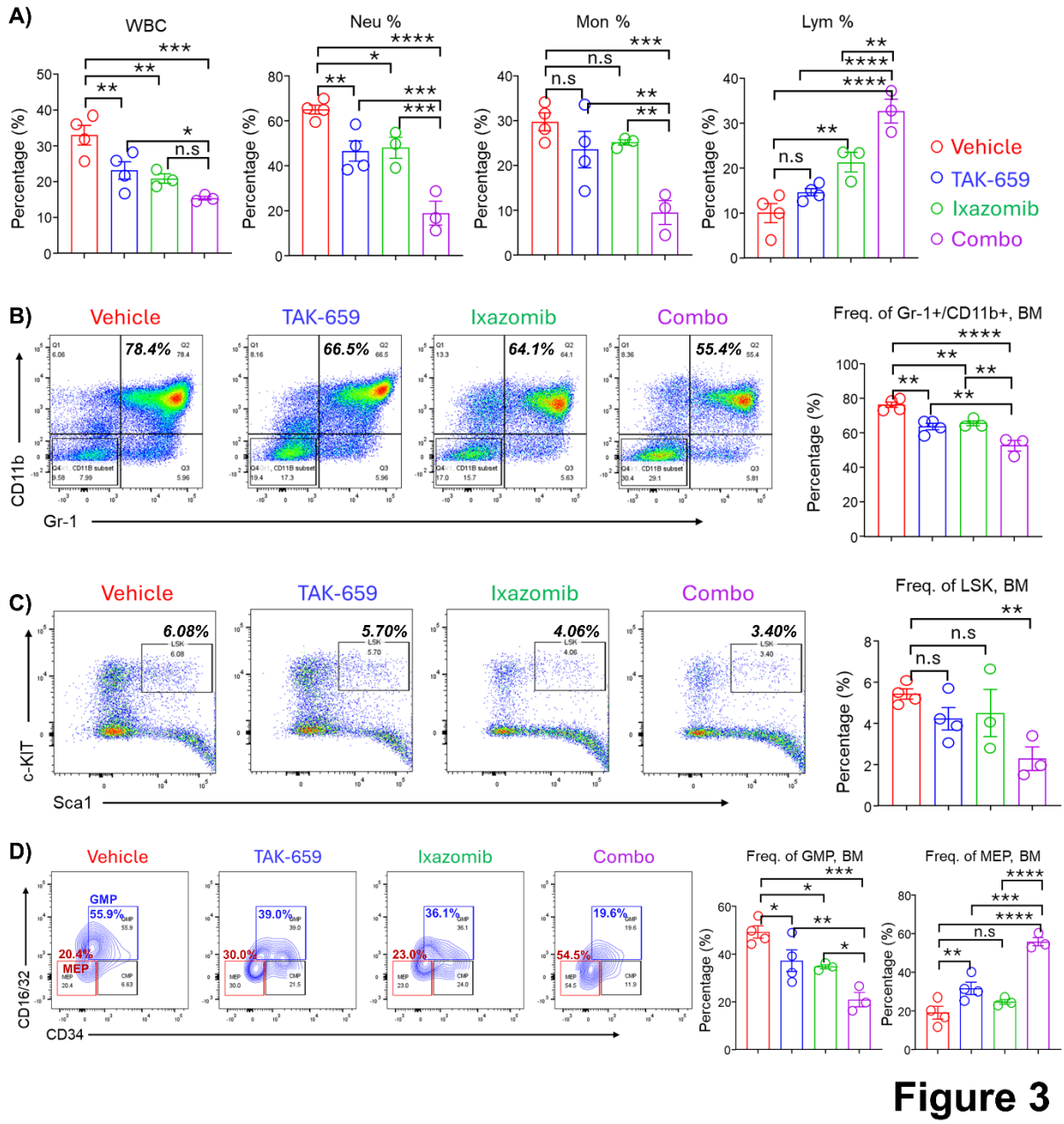

Figure 3

Figure 3. Combination of TAK-659 and Ixazomib reduces leukemic burden and restores normal hematopoiesis in wild-type (WT) mice transplanted with *Tet2*$^{-/-}$;*Flt3*^{ITD} AML cells.

A) Peripheral blood differential counts showing normalization of white blood cells (WBCs), neutrophils (Neu), monocytes (Mon), and lymphocytes (Lym) following combination therapy. **B)** Flow cytometry analysis and quantification of BM myeloid populations (Gr-1^{+}/CD11b^{+}), demonstrating reduced leukemic myeloid expansion in the combination group. **C)** Frequencies of hematopoietic stem/progenitor cells (LSK; Lin^{-}Sca1^{+}c-Kit^{+}) in BM, showing a significant reduction

following dual treatment compared with vehicle. **D)** Representative plots and quantification of granulocyte macrophage progenitors (GMPs; c-Kit^{+}CD16/32^{+}CD34^{+}) and megakaryocyte erythroid progenitors (MEPs), revealing decreased GMPs and increased MEPs after combination therapy, indicative of restored differentiation potential. Data are presented as mean ± SEM. Statistical significance was determined by one-way ANOVA with Tukey's multiple-comparison test. *$p < 0.05$, **$p < 0.01$, ***$p < 0.001$, ****$p < 0.0001$; n.s. not significant.

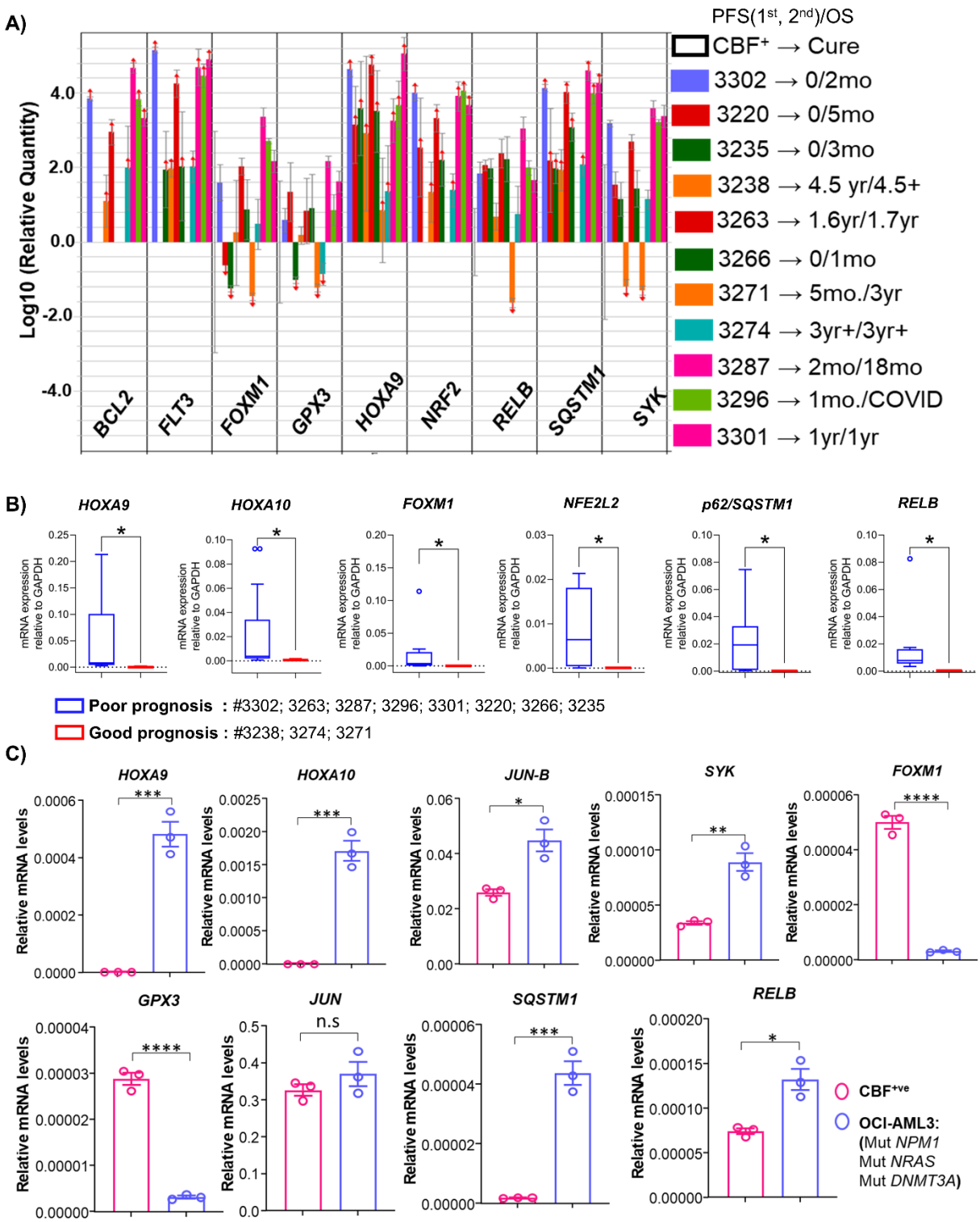
A)
PFS(1st, 2nd)/OS
CBF+ → Cure
3302 → 0/2mo
3220 → 0/5mo
3235 → 0/3mo
3238 → 4.5 yr/4.5+
3263 → 1.6yr/1.7yr
3266 → 0/1mo
3271 → 5mo./3yr
3274 → 3yr+/3yr+
3287 → 2mo/18mo
3296 → 1mo./COVID
3301 → 1yr/1yr
Log10 (Relative Quantity)
BCL2
FLT3
FOXM1
GPX3
HOXA9
NRF2
RELB
SQSTM1
SYK
B)
HOXA9
HOXA10
FOXM1
NFE2L2
p62/SQSTM1
RELB
mRNA expression relative to GAPDH
Poor prognosis : #3302; 263; 3287; 3296; 3301; 3220; 3266; 3235
Good prognosis : #3238; 3274; 3271
C)
HOXA9
HOXA10
JUN-B
SYK
FOXM1
GPX3
JUN
n.s
SQSTM1
RELB
Relative mRNA levels
CBF+ve
OCI-AML3:
(Mut NPM1
Mut NRAS
Mut DNMT3A)

Figure 4

Figure 4: High expression of developmental and stress-adaptive transcriptional genes correlates with poor prognosis outcomes in AML.

A) Relative mRNA expression levels were quantified for *BCL2, FLT3, FOXM1, GPX3, HOXA9, NRF2, RELB, SQSTM1*, and *SYK* using TaqMan assays on a cohort of patient blast cells (n=11). Notably, a distinct group of samples from patients exhibiting prolonged progression-free survival. **B)** Relative mRNA expression levels of *HOXA9, FOXM1, NRF2, p62/SQSTM1,* and *RELB* between patients with poor and good prognosis based on the progression free survival (PFS) and overall survival parameters. **C)** The quantitative expression of prognostic genes was compared between *CBF*$^{+ve}$ sample and the OCI-AML3 cell line, which harbors mutant *NPM1, NRAS,* and *DNMT3A*. Data was analyzed using $2^{-\Delta Ct}$ approach, normalized to the endogenous control GAPDH and represented as an average with standard deviation. Two-tailed Unpaired t-test was applied to determine the statistical significance (*p<0.05, **p<0.01, ***p<0.001, ****p<0.0001).

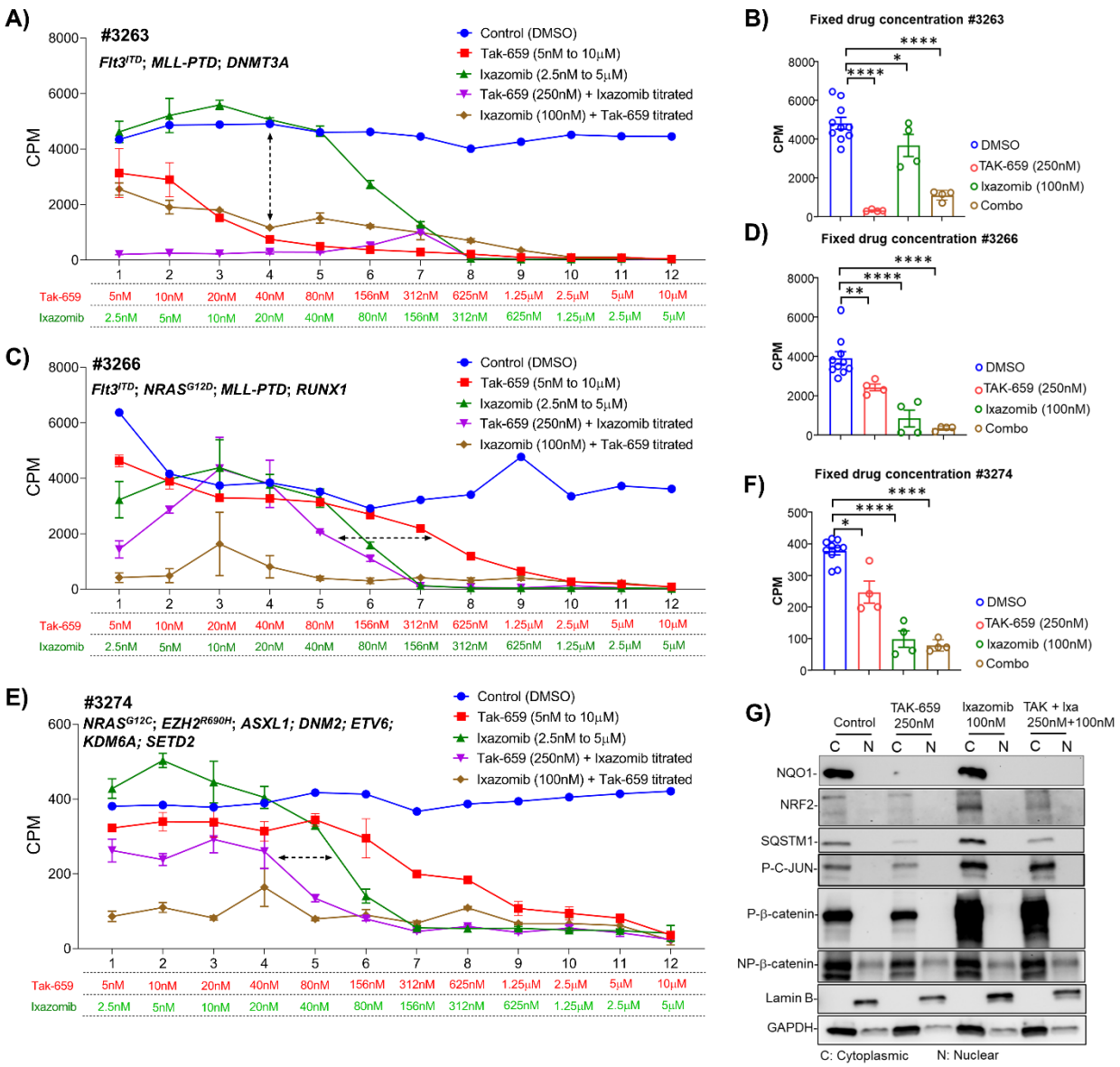

Figure 5

Figure 5: Mutational landscape determines differential therapeutic sensitivity on genetically diverse primary AML blasts and stress-adaptive reprogramming. The AML blasts from the patients **A-B)** #3263 (*FLT3*^{ITD}, *MLL-PTD*, *DNMT3A* mutated), **C-D)** #3266 (*FLT3*^{ITD}, *NRAS*^{G12D}, *MLL-PTD*, *RUNX1* mutated) and **E-F)** #3274 (*NRAS*^{ITD}, *EZH2*^{R690H}, *ASXL1*, *DNM2*, *ETV6*, *KDM6A*, *SETD2* mutated) were treated with the varying concentrations (two-fold) of TAK-659 and Ixazomib in the *in vitro* for 48 hours. DMSO treated cells were used as a control. Line plots illustrate the dose dependent concentrations effects on the AML blast cells. Bar plots depict the specific IC_{50} concentrations of TAK-659 and Ixazomib in alone or combination. The

combination treatments were performed using TAK-659 (250nM; IC50) as a constant across the two-fold diluted concentrations of the Ixazomib. Likewise, the cells were treated with the Ixazomib (100nM; IC50) across the two-fold diluted concentrations of TAK-659. Data was represented as an average of counts per minute (CPM) with standard deviation for the indicated concentrations. **G)** Western blot analysis of cytosolic and nuclear extracts of AML blasts cells treated with TAK-659 (250nM), Ixazomib (100nM) and in combination. GAPDH and Lamin-B were used as endogenous controls for the cytosol and nuclear content respectively.

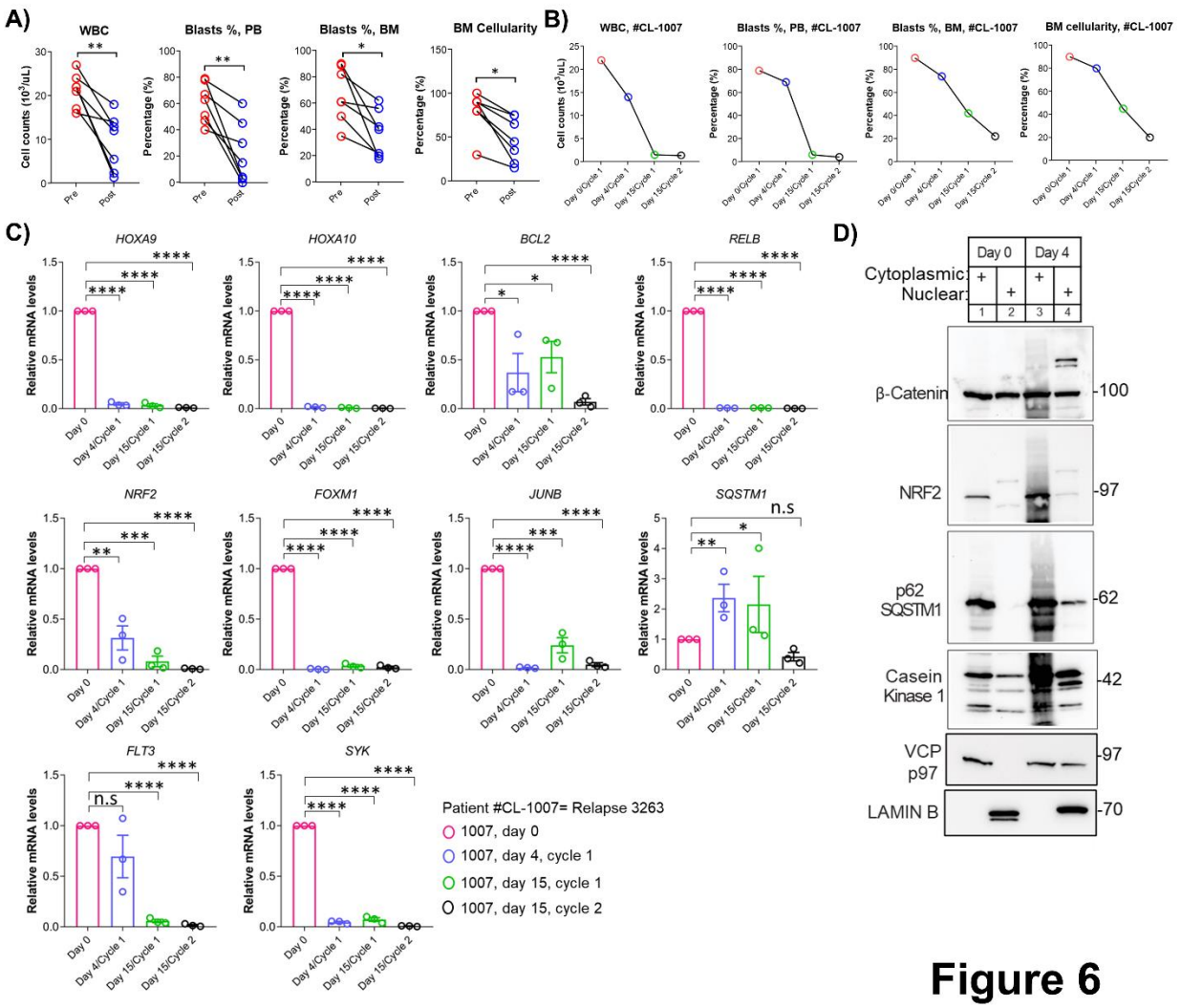

Figure 6

Figure 6: Clinical and molecular response to dual FLT3/SYK and proteasome inhibition in AML patients. A) Pre- and post-treatment clinical observations of WBC counts (10^3/μL), peripheral blood and bone marrow blast percentage, bone marrow cellularity in the AML patients. Two-tailed Paired-test (*p<0.05, **p<0.01). **B)** Clinical response of AML patient (#CL-1007) enrolled in the study with respect to the WBC counts, peripheral blood and bone marrow blasts, bone marrow cellularity over a duration of treatment. **C)** Relative mRNA expression profiles of *HOXA9, HOXA10, BCL2, RELB, NRF2, FOXM1, JUNB, SQSTM1, FLT3,* and *SYK* in the patient treated (#CL-1007) over a course of duration during the study period. Data was analyzed using $2^{-\Delta\Delta Ct}$ approach, normalized to the endogenous control GAPDH and represented as an average with standard deviation compared to the pre-treated (Day 0) patient AML bone marrow blast samples. One-way ANOVA with Posthoc Tukey's test was applied to determine the statistical significance (*p<0.05, **p<0.01, ***p<0.001, ****p<0.0001, ns – not significant). **D)** Western blot analysis of patient (#CL-1007) bone marrow blasts before (Day 0) and on the following 4th day

treatment with the TAK-659 and Ixazomib combination on protocol BTCRC-HEME17-092. Lamin B was used as a loading control.

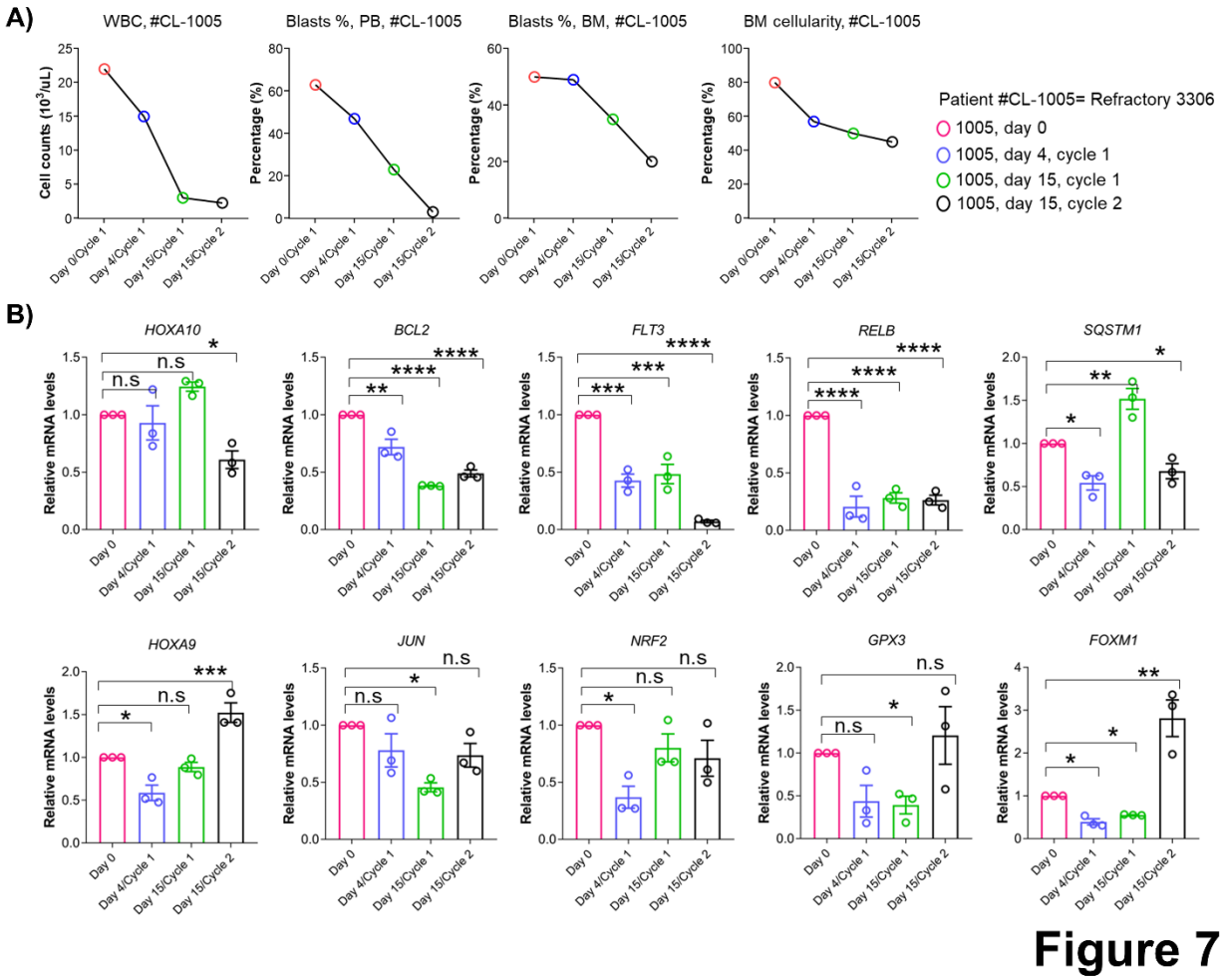

Figure 7

Figure 7: Coordinated hematologic improvement and repression of leukemogenic and stress-adaptive transcriptional programs following dual FLT3/SYK and proteasome inhibition AML patient #CL-1005. A) The quantitative estimation of WBC counts, peripheral blood and bone marrow blasts, bone marrow cellularity in the AML patient (#CL-1005, *TET2*, *SRSF2* mutated) enrolled in the study over a duration of treatment. **B)** Relative mRNA expression of *HOXA10, BCL2, FLT3, RELB, SQSTM1, HOXA9, JUN, NRF2, GPX3* and *FOXM1* in the bone marrow blasts of the patient (#CL-1005) under treatment, over a course of duration during the study enrollment. Data was analyzed using $2^{-\Delta\Delta Ct}$ approach, normalized to the endogenous control GAPDH and represented as an average with standard deviation compared to the pre-treated (Day 0) patient AML bone marrow blast samples. One-way ANOVA with Posthoc Tukey's test was applied to determine the statistical significance (*p<0.05, **p<0.01, ***p<0.001, ****p<0.0001, ns – not significant).

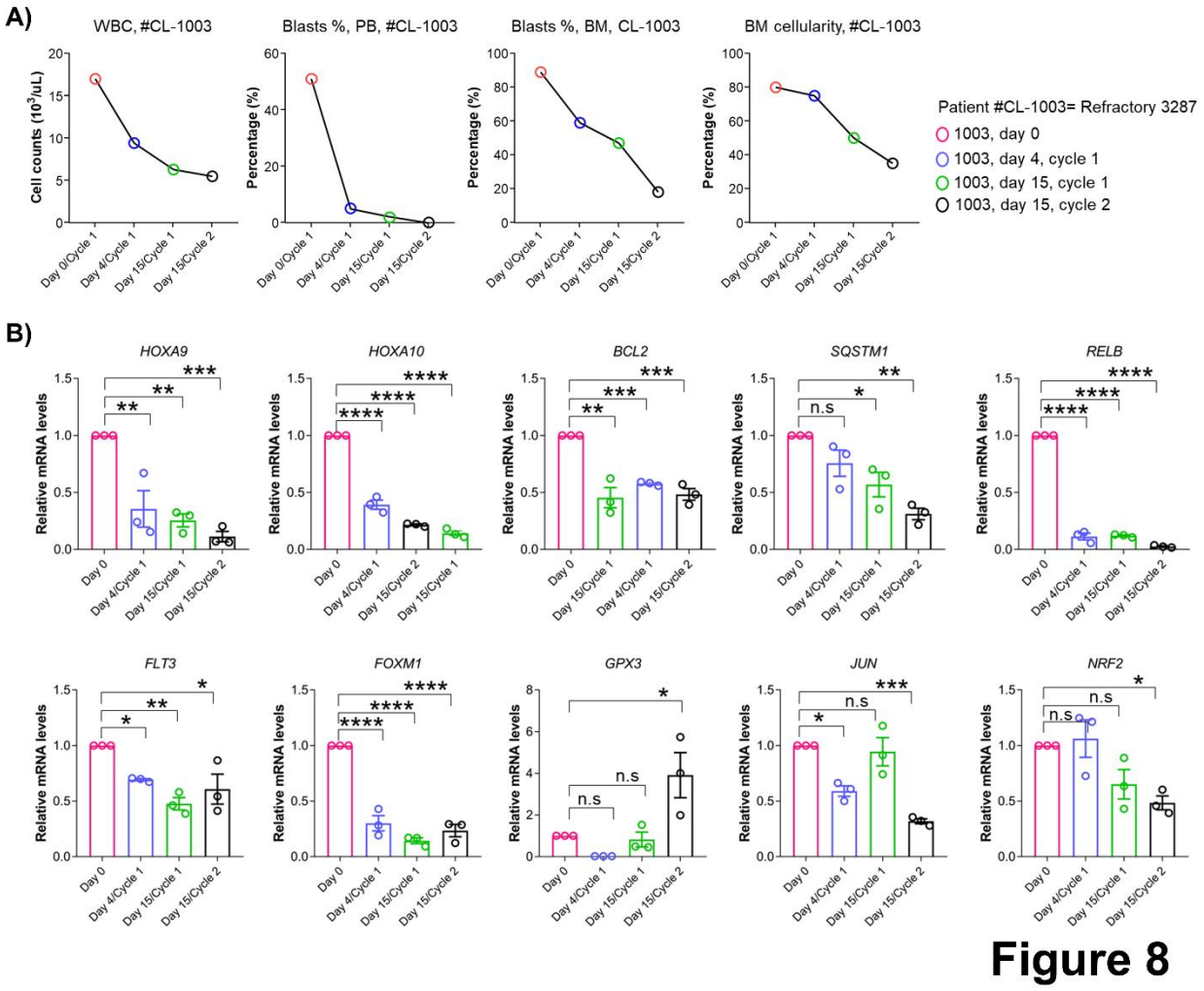

Figure 8

Figure 8: Temporal decline in leukemic burden and transcriptional activity following TAK-659 + Ixazomib treatment in AML patient #CL-1003. A) Clinical profile of WBC counts, peripheral blood and bone marrow blasts, bone marrow cellularity in the AML patient (#CL-1003) enrolled in the study. **B)** Relative mRNA expression of HOXA9, *HOXA10, BCL2, SQSTM1, RELB, FLT3, FOXM1, GPX3, JUN* and *NRF2* in the bone marrow blasts of the patient (#CL-1003) over a course of treatment during the study enrollment. Data was analyzed using $2^{-\Delta\Delta Ct}$ approach, normalized to the endogenous control GAPDH and represented as an average with standard deviation compared to the pre-treated (Day 0) patient AML bone marrow blast samples. One-way ANOVA with Posthoc Tukey's test was applied to determine the statistical significance (*p<0.05, **p<0.01, ***p<0.001, ****p<0.0001, ns – not significant).

Graphical abstract:

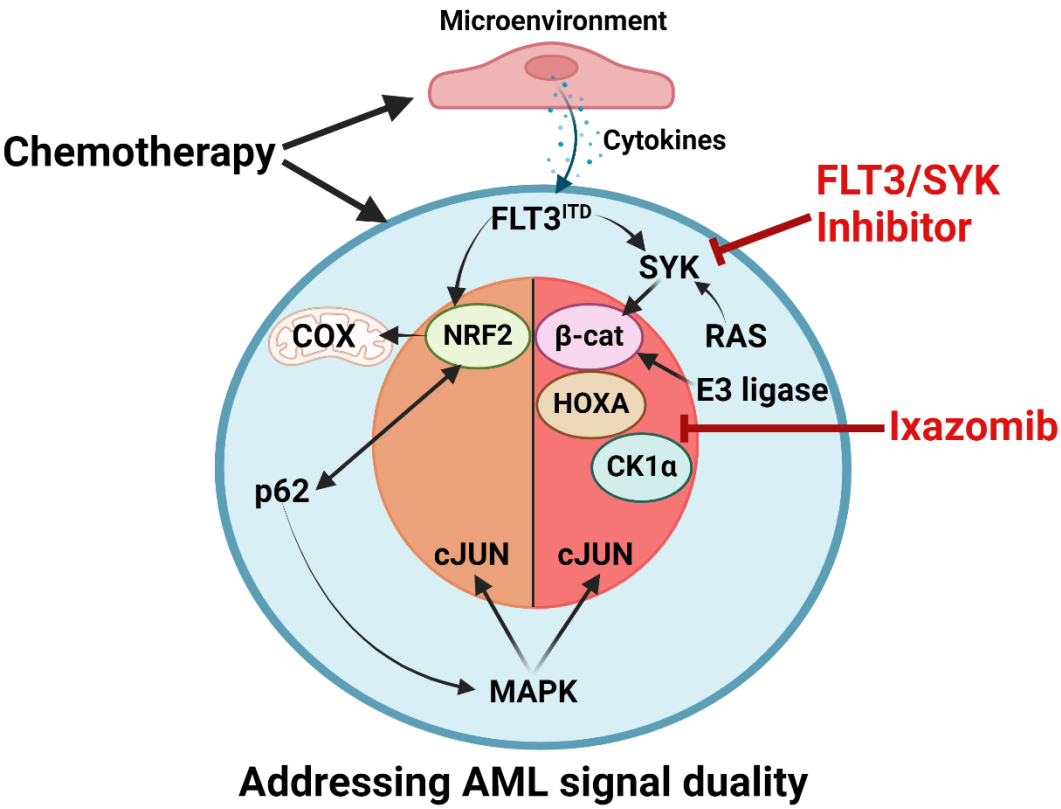

Table: 1. Phase I/II Clinical Trial Outcomes of TAK-659 and Ixazomib Combination Therapy in Relapsed or Refractory AML

Patient #	Cycle/Day	WBC ($10^3/\mu L$)	PB‡ Blast Percentage	BM‡ Blast Percentage	BM‡ cellularity	PFS/OS
CL-1001	1/1	27	67%	61%	90%	Progression
	1/4	25	65%	58%	85%	
	1/15	15	55%	55%	66%	
	2/15	12.9	45%	42%	65%	
CL-1003	1/1	17	51%	89%	80%	2mo/18mo
	1/4	9.4	5%	59%	75%	
	1/15	6.3	2%	47%	50%	
	2/15	5.5	0%	18%	35%	
CL-1004	1/1	21	47%	61%	30%	NE/1mo
	1/4	20	33%	42%	20%	
	1/15	17	18%	38%	10%	
	2/15	12	15%	56%	15%	
CL-1005	1/1	22	63%	50%	80%	4.5mo/7.5mo
	1/4	15	47%	49%	57%	
	1/15	3	23%	35%	50%	
	2/15	2.3	3%	20%	45%	
CL-1006	1/1	16	40%	35%	90%	2mon/5mon
	1/4	15	20%	30%	90%	
	1/15	10	35%	25%	85%	
	2/15	14	30%	22%	75%	
CL-1007	1/1	22	79%	90%	90%	5mo/8.5mo
	1/4	14	69%	74%	80%	
	1/15	1.5	6%	42%	45%	
	2/15	1.4	4%	22%	20%	
CL-1008	1/1	24	78%	82%	100%	1mo/1mo
	1/4	20	77%	80%	100%	
	1/15	20	83%	72%	85%	
	2/15	18	60%	62%	75%	

‡**Note:** NE: Not Evaluated; PB: peripheral blood; BM: bone marrow; mo: month; PFS: Progression free survival; OS: Overall survival